nature neuroscience

Supplementary information

https://doi.org/10.1038/s41593-026-02359-0

The cross-site reproducibility of MRI morphometric phenotypes in psychiatric disorders

In the format provided by the authors and unedited

1 Supplementary Tables

Supplementary Table 1. Summary of datasets used in this study.

Dataset	Accessibility
Autism Brain Imaging Data Exchange I (ABIDE I)[1,2]	Available in the ABIDE I repository, http://fcon_1000.projects.nitrc.org/indi/abide/abide_I.html
Autism Brain Imaging Data Exchange (ABIDE II)[3]	Available in the ABIDE II repository, http://fcon_1000.projects.nitrc.org/indi/abide/abide_II.html
Australian Imaging, Biomarker & Lifestyle (AIBL)[4,5]	Available in the AIBL repository, subject to the approval of the AIBL Management Committee https://aibl.org.au/ https://ida.loni.usc.edu/
Advancing innovative brain imaging to detect altered glutamate modulation and network dynamics in schizophrenia (AIS*)[6]	Available on NDA, subject to the approval of Data Access Committee https://nda.nih.gov/edit_collection.html?id=2488
Bipolar & Schizophrenia Consortium for Parsing Intermediate Phenotypes (B-SNIP 1)[7]	Available on NDA, subject to the approval of Data Access Committee https://nda.nih.gov/edit_collection.html?id=2274
Bipolar & Schizophrenia Consortium for Parsing Intermediate Phenotypes (B-SNIP 2)	Available on NDA, subject to the approval of Data Access Committee https://nda.nih.gov/edit_collection.html?id=2165
The Autistic Brain Over 45: The Anatomic, Functional, and Cognitive Phenotype(ASD45*)[8]	Available on NDA, subject to the approval of Data Access Committee https://nda.nih.gov/edit_collection.html?id=2291
Glutamatergic and Neuronal Dysfunction in Gray and White Matter (BrainGluSchi)[9]	Available in the BrainGluSchi repository, http://schizconnect.org/
The Center for Biomedical Research Excellence (COBRE)[10]	Available in the COBRE repository, http://fcon_1000.projects.nitrc.org/indi/retro/cobre.html
The Determinants of Social Disconnectedness: A Spectrum from the General Community to Severe Mental Illness(DSD*)[11]	Available on NDA, subject to the approval of Data Access Committee https://nda.nih.gov/edit_collection.html?id=2481
Human Connectome Project for Early Psychosis (HCP-EP)[12]	Available on NDA, subject to the approval of Data Access Committee https://www.humanconnectome.org/study/human-connectome-project-for-early-psychosis https://nda.nih.gov/edit_collection.html?id=2914

Singapore Memory Ageing and Cognition Centre (MACC) Harmonization Project (Harmonization)[13–15]	Available from the principal investigator of the study, subject to local ethics committee requirements
Inhibitory dysfunction in autism (IDAUT*)[16,17]	Available on NDA, subject to the approval of Data Access Committee https://nda.nih.gov/edit_collection.html?id=2266
Monash Brain and Behaviour Project (MBBP)	Available from the principal investigator of the study, subject to local ethics committee requirements
MIND Clinical Imaging Consortium (MCIC)[18]	Available in the MCIC repository, http://schizconnect.org/
Modulation of ventrolateral prefrontal cortical activity during reward processing by transcranial direct current stimulation (MRITDCS*)[19]	Available on NDA, subject to the approval of Data Access Committee https://nda.nih.gov/edit_collection.html?id=2432
A Multidimensional Investigation of Cognitive Control Deficits in Psychopathology (MICCD*)[20]	Available on NDA, subject to the approval of Data Access Committee https://nda.nih.gov/edit_collection.html?id=2102
Cortical myelin measured by the T1w/T2w ratio in individuals with depressive disorders and healthy controls (Myelin*)[21]	Available in the repository https://openneuro.org/datasets/ds003653/versions/1.0.0
Open Access Series of Imaging Studies (OASIS-3)[22]	Available on OASIS repository, subject to the approval of Knight ADRC https://www.oasis-brains.org
Open Access Series of Imaging Studies (OASIS-4)[23]	Available on OASIS repository, subject to the approval of Knight ADRC https://www.oasis-brains.org
Psychosis and Affective Research Domains and Intermediate Phenotypes (PARDIP)[24,25]	Available on NDA, subject to the approval of Data Access Committee https://nda.nih.gov/edit_collection.html?id=2126
Resting state with closed eyes for patients with depression and healthy participants (RD*)[26]	Available in the repository https://openneuro.org/datasets/ds002748/versions/1.0.5
Japanese Strategic Research Program for the Promotion of Brain Science (SRPBS)[27,28]	Available in the SRPBS repository, subject to the approval of the DecNef Consortium https://bicr.atr.jp/decnefpro/data/
Specificity of Hippocampal Subregion Cerebral Blood Volume Abnormalities in Psychiatric Disorders (SHSCBV*)[29]	Available on NDA, subject to the approval of Data Access Committee https://nda.nih.gov/edit_collection.html?id=3199

A Study of the neural and psychological correlates of emotion and motivation processing deficits in individuals with schizophrenia vs. controls (EMOSCZ*)[30,31]	Available on NDA, subject to the approval of Data Access Committee https://nda.nih.gov/edit_collection.html?id=2703
The Transdiagnostic Connectome Project (TCP)[32]	Available in the repository https://openneuro.org/datasets/ds005237
UCLA Consortium for Neuropsychiatric Phenomics (UCLA-CNP)[33,34]	Available in the UCLA repository https://openneuro.org/datasets/ds000030/versions/00016
Youth Depression Alleviation-Combined Treatment (YoDA)[35,36]	Available from the principal investigator of the study, subject to local ethics committee requirements
Minimal Interval Resonance Imaging in Alzheimer's Disease (MIRIAD)[37]	Available in the MIRIAD repository, https://www.ucl.ac.uk/drc/research-clinical-trials/minimal-interval-resonance-imaging-alzheimers-disease-miriad
Brain correlates of speech perception in schizophrenia patients with and without auditory hallucinations (Speech*)[38]	Available in the repository https://openneuro.org/datasets/ds004302/versions/1.0.0

*short names for the datasets.

Supplementary Table 2. Summary of data for each disorder in the VBM analysis.

Note that some sites have multiple disorders and the controls are the same for different disorders in these sites.

Disorder	Number of sites	Number of cases (male)	Number of controls (male)
AD	7	603 (249)	732 (301)
SCZ	17	800 (531)	964 (543)
SCA	6	187 (91)	307 (121)
ASD	5	249 (210)	250 (212)
MDD	8	397 (167)	466 (183)
BD	9	307 (137)	530 (256)

Supplementary Table 3. Summary of demographics for each site used in the SBM analysis.

Disorder	Index	Site	Dataset	Control No (%male)	Control Age(year) median (SD) [range]	Case No (%male)	Case Age(year) median (SD) [range]
AD	1	AIBL-2	AIBL	160 (43)	73 (7) [61 92]	30 (40)	78 (7) [59 93]
AD	2	Harmonisation	Harmonisation	132 (45)	69 (8) [50 89]	192 (31)	76 (7) [55 91]
AD	3	MIRIAD	MIRIAD	23 (52)	68 (7) [58 86]	45 (40)	69 (7) [56 86]
AD	4	OASIS3-3	OASIS3	237 (39)	72 (9) [46 95]	127 (52)	77 (7) [59 96]
AD	5	OASIS3-4	OASIS3	167 (43)	68 (8) [43 93]	36 (58)	77 (8) [51 92]
AD	6	OASIS3-5	OASIS3	187 (40)	72 (8) [46 92]	37 (41)	76 (7) [60 90]
AD	7	OASIS4	OASIS4	31 (45)	66 (8) [46 85]	187 (42)	75 (8) [49 94]
SCZ	1	AIS	AIS	28 (64)	26 (6) [19 42]	40 (75)	28 (9) [18 50]

SCZ	2	BrainGluSchi	BrainGluSchi	60 (77)	38 (12) [18 60]	64 (88)	32 (12) [19 60]
SCZ	3	Baltimore	BSNIP	55 (42)	49 (11) [25 59]	74 (73)	35 (12) [18 57]
SCZ	4	Boston2	BSNIP	25 (48)	31 (11) [18 58]	25 (64)	28 (12) [19 57]
SCZ	5	Dallas2	BSNIP	58 (47)	40 (12) [18 60]	21 (62)	42 (10) [21 56]
SCZ	6	Hartford2	BSNIP	48 (35)	30 (12) [19 60]	51 (75)	27 (10) [18 57]
SCZ	7	Boston1	BSNIP2	43 (47)	28 (10) [21 58]	48 (71)	32 (13) [18 60]
SCZ	8	Chicago	BSNIP2	67 (42)	35 (10) [19 58]	48 (56)	41 (10) [21 60]
SCZ	9	Dallas1	BSNIP2	36 (33)	30 (10) [21 56]	38 (50)	39 (11) [22 58]
SCZ	10	Georgia	BSNIP2	73 (26)	39 (13) [18 60]	23 (74)	38 (11) [18 58]
SCZ	11	Hartford1	BSNIP2	32 (59)	26 (13) [18 60]	22 (50)	41 (13) [19 59]
SCZ	12	COBRE	COBRE	71 (68)	34 (11) [18 58]	66 (80)	34 (12) [18 57]
SCZ	13	DSD	DSD	25 (68)	49 (11) [20 60]	26 (65)	53 (11) [28 60]
SCZ	14	HCP-EP	HCP-EP	27 (74)	24 (4) [20 36]	69 (54)	22 (4) [18 35]
SCZ	15	MCIC-A	MCIC	43 (79)	23 (12) [18 54]	43 (77)	28 (12) [18 60]
SCZ	16	MCIC-C	MCIC	22 (59)	26 (13) [18 60]	28 (71)	28 (10) [18 56]
SCZ	17	MCIC-D	MCIC	23 (57)	43 (9) [20 50]	26 (77)	40 (9) [20 50]
SCZ	18	MICCD	MICCD	62 (69)	32 (8) [20 54]	86 (64)	31 (9) [18 50]
SCZ	19	Speech	Speech	22 (68)	36 (14) [20 60]	43 (79)	42 (9) [19 60]
SCZ	20	KTT	SRPBS	73 (66)	28 (9) [19 57]	45 (53)	38 (10) [24 57]
SCZ	21	KUT	SRPBS	125 (58)	38 (12) [18 60]	39 (46)	40 (9) [20 55]
SCZ	22	UTO	SRPBS	145 (50)	23 (11) [19 60]	34 (68)	31 (10) [18 52]
SCZ	23	EMOSCZ	EMOSCZ	49 (49)	36 (9) [21 51]	71 (66)	38 (9) [22 50]
SCZ	24	UCLA1	UCLA	81 (53)	29 (9) [21 50]	24 (67)	40 (9) [22 49]
SCA	1	Baltimore	BSNIP	55 (42)	49 (11) [25 59]	28 (50)	30 (10) [18 52]
SCA	2	Dallas2	BSNIP	58 (47)	40 (12) [18 60]	37 (41)	40 (11) [18 57]
SCA	3	Hartford2	BSNIP	48 (35)	30 (12) [19 60]	42 (43)	38 (12) [18 57]
SCA	4	Boston1	BSNIP2	43 (47)	28 (10) [21 58]	22 (55)	42 (13) [18 56]
SCA	5	Chicago	BSNIP2	67 (42)	35 (10) [19 58]	49 (41)	40 (12) [20 60]
SCA	6	Dallas1	BSNIP2	36 (33)	30 (10) [21 56]	33 (61)	44 (12) [21 58]
SCA	7	Georgia	BSNIP2	73 (26)	39 (13) [18 60]	27 (52)	41 (12) [20 56]
SCA	8	Hartford1	BSNIP2	32 (59)	26 (13) [18 60]	34 (47)	49 (12) [22 59]
ASD	1	USM	ABIDEI	29 (100)	25 (6) [18 39]	39 (100)	24 (8) [18 50]
ASD	2	BNI	ABIDEII	27 (100)	43 (14) [18 60]	26 (100)	32 (15) [18 57]
ASD	3	ASD45	ASD45	31 (87)	51 (5) [40 59]	23 (70)	48 (6) [40 61]
ASD	4	IDAUT	IDAUT	35 (60)	22 (3) [19 31]	26 (62)	22 (4) [18 31]
ASD	5	SWA	SRPBS	100 (85)	26 (8) [19 55]	115 (87)	30 (8) [20 54]
MDD	1	MBBP	MBBP	80 (42)	28 (8) [18 45]	62 (24)	26 (8) [18 45]
MDD	2	Myelin	Myelin	47 (23)	28 (6) [19 44]	39 (26)	28 (7) [19 44]
MDD	3	RD	RD	21 (29)	31 (8) [22 52]	50 (26)	31 (9) [19 55]
MDD	4	COI	SRPBS	85 (34)	46 (9) [20 60]	56 (46)	41 (8) [27 58]
MDD	5	HKH	SRPBS	27 (41)	45 (8) [28 60]	28 (64)	42 (9) [25 57]
MDD	6	HUH	SRPBS	63 (41)	31 (11) [20 60]	52 (56)	40 (9) [26 58]
MDD	7	UTO	SRPBS	145 (50)	23 (11) [19 60]	60 (60)	38 (11) [18 60]
MDD	8	YoDA	YoDA	78 (44)	21 (2) [18 26]	115 (48)	21 (2) [18 26]
BD	1	Baltimore	BSNIP	55 (42)	49 (11) [25 59]	28 (29)	37 (12) [18 56]
BD	2	Boston2	BSNIP	25 (48)	31 (11) [18 58]	28 (32)	36 (11) [20 59]
BD	3	Dallas2	BSNIP	58 (47)	40 (12) [18 60]	25 (28)	41 (10) [21 60]
BD	4	Hartford2	BSNIP	48 (35)	30 (12) [19 60]	28 (50)	36 (13) [19 60]
BD	5	Chicago	BSNIP2	67 (42)	35 (10) [19 58]	48 (42)	28 (10) [18 59]
BD	6	DSD	DSD	25 (68)	49 (11) [20 60]	20 (50)	49 (10) [22 60]
BD	7	MRITDCS	MRITDCS	38 (34)	26 (6) [19 44]	32 (34)	28 (9) [19 46]
BD	8	MICCD	MICCD	62 (69)	32 (8) [20 54]	40 (50)	32 (10) [20 49]
BD	9	PARDIP1	PARDIP	22 (36)	36 (12) [23 58]	38 (37)	49 (9) [26 59]

BD	10	PARDIP2	PARDIP	28 (54)	28 (11) [19 56]	20 (50)	36 (10) [20 52]
BD	11	SHSCBV	SHSCBV	30 (50)	31 (6) [26 48]	24 (46)	32 (9) [26 53]
BD	12	UTO	SRPBS	145 (50)	23 (11) [19 60]	41 (63)	33 (9) [19 56]
BD	13	Transdiagnostic2	TCP	31 (45)	32 (11) [19 60]	22 (50)	33 (12) [19 58]
BD	14	UCLA1	UCLA	81 (53)	29 (9) [21 50]	26 (46)	36 (10) [22 50]

Supplementary Table 4. Summary of demographics for each site used in the VBM analysis.

Disorder	**Index**	**Site**	**Dataset**	**Control No (%male)**	**Control Age(year) median (SD) [range]**	**Case No (%male)**	**Case Age(year) median (SD) [range]**
AD	1	AIBL-2	AIBL	152 (43)	73 (7) [61 92]	27 (41)	73 (7) [59 85]
AD	2	Harmonisation	Harmonisation	117 (44)	68 (8) [50 89]	164 (30)	75 (7) [55 91]
AD	3	OASIS3-3	OASIS3	245 (37)	71 (9) [46 95]	119 (50)	76 (7) [59 96]
AD	4	OASIS3-4	OASIS3	85 (42)	68 (9) [43 93]	31 (55)	76 (8) [51 92]
AD	5	OASIS3-5	OASIS3	82 (41)	72 (8) [46 89]	28 (43)	76 (7) [60 88]
AD	6	OASIS4	OASIS4	31 (42)	66 (8) [46 80]	196 (43)	75 (8) [49 94]
AD	7	MIRIAD	MIRIAD	20 (50)	68 (7) [58 86]	38 (42)	69 (7) [56 86]
SCZ	1	MCIC-A	MCIC	24 (83)	25 (11) [18 54]	20 (70)	25 (10) [18 51]
SCZ	2	AIS	AIS	34 (68)	26 (6) [19 46]	48 (73)	29 (9) [18 50]
SCZ	3	Baltimore	BSNIP	54 (43)	49 (11) [25 59]	63 (75)	35 (12) [18 57]
SCZ	4	BrainGluSchi	BrainGluSchi	33 (64)	31 (11) [18 60]	26 (88)	27 (10) [19 51]
SCZ	5	MCIC-C	MCIC	26 (58)	28 (12) [18 60]	27 (74)	27 (10) [18 56]
SCZ	6	COBRE	COBRE	68 (68)	34 (10) [18 58]	58 (83)	34 (12) [18 57]
SCZ	7	Dallas2	BSNIP	58 (47)	40 (12) [18 60]	20 (60)	42 (10) [21 56]
SCZ	8	HCP-EP	HCP-EP	55 (67)	24 (4) [19 36]	108 (62)	22 (4) [18 35]
SCZ	9	KTT	SRPBS	71 (65)	28 (9) [19 57]	44 (52)	37 (10) [22 57]
SCZ	10	KUT	SRPBS	150 (59)	35 (12) [18 60]	41 (44)	40 (8) [23 55]
SCZ	11	MICCD	MICCD	35 (69)	34 (9) [20 54]	48 (65)	29 (7) [18 50]
SCZ	12	EMOSCZ	EMOSCZ	48 (48)	37 (9) [21 51]	61 (67)	38 (8) [22 50]
SCZ	13	UTO	SRPBS	111 (50)	25 (11) [19 60]	28 (71)	35 (10) [18 52]
SCZ	14	Boston1	BSNIP2	40 (48)	28 (10) [21 58]	42 (71)	32 (12) [19 60]
SCZ	15	Chicago	BSNIP2	65 (40)	35 (10) [19 58]	45 (56)	41 (10) [21 60]
SCZ	16	Dallas1	BSNIP2	36 (33)	30 (10) [21 56]	38 (50)	39 (11) [22 58]
SCZ	17	Speech	Speech	21 (67)	36 (13) [20 60]	35 (77)	41 (10) [20 60]
SCA	1	Baltimore	BSNIP	54 (43)	49 (11) [25 59]	24 (50)	29 (10) [18 52]
SCA	2	Dallas2	BSNIP	58 (47)	40 (12) [18 60]	36 (42)	39 (11) [18 57]
SCA	3	Chicago	BSNIP2	65 (40)	35 (10) [19 58]	46 (41)	40 (11) [20 60]
SCA	4	Dallas1	BSNIP2	36 (33)	30 (10) [21 56]	33 (61)	44 (12) [21 58]
SCA	5	Georgia	BSNIP2	64 (23)	38 (13) [18 60]	21 (57)	41 (12) [20 56]
SCA	6	Hartford1	BSNIP2	30 (60)	28 (13) [18 60]	27 (48)	49 (12) [22 59]
ASD	1	BNI	ABIDEII	27 (100)	43 (14) [18 60]	28 (100)	40 (16) [18 59]
ASD	2	ASD45	ASD45	29 (86)	51 (6) [40 59]	20 (65)	48 (7) [40 61]
ASD	3	IDAUT	IDAUT	38 (61)	22 (4) [19 31]	29 (66)	22 (4) [18 31]
ASD	4	SWA	SRPBS	99 (85)	26 (7) [19 55]	113 (87)	30 (8) [20 54]
ASD	5	USM	ABIDEI	28 (100)	24 (6) [18 39]	39 (100)	24 (8) [18 50]
MDD	1	COI	SRPBS	56 (29)	45 (9) [22 60]	30 (43)	39 (7) [27 58]
MDD	2	HKH	SRPBS	26 (42)	44 (9) [28 60]	25 (64)	43 (9) [25 57]
MDD	3	HUH	SRPBS	63 (41)	31 (11) [20 60]	51 (55)	40 (9) [26 58]
MDD	4	MBBP	MBBP	81 (42)	28 (8) [18 45]	64 (25)	26 (8) [18 45]

MDD	5	Myelin	Myelin	46 (24)	27 (6) [19 44]	39 (26)	28 (7) [19 44]
MDD	6	RD	RD	21 (29)	31 (8) [22 52]	46 (28)	31 (9) [19 55]
MDD	7	UTO	SRPBS	111 (50)	25 (11) [19 60]	53 (60)	40 (11) [20 60]
MDD	8	YoDA	YoDA	62 (39)	21 (2) [18 26]	89 (44)	21 (2) [18 26]
BD	1	Baltimore	BSNIP	54 (43)	49 (11) [25 59]	24 (25)	37 (12) [18 56]
BD	2	Dallas2	BSNIP	58 (47)	40 (12) [18 60]	25 (28)	41 (10) [21 60]
BD	3	MRITDCS	MRITDCS	43 (40)	26 (6) [19 44]	34 (35)	28 (8) [19 46]
BD	4	MICCD	MICCD	35 (69)	34 (9) [20 54]	32 (56)	33 (10) [20 49]
BD	5	PARDIP1	PARDIP	22 (36)	36 (12) [23 58]	38 (37)	49 (9) [26 59]
BD	6	Transdiagnostic2	TCP	30 (43)	33 (11) [19 60]	21 (52)	32 (12) [19 58]
BD	7	UCLA1	UCLA	77 (51)	29 (9) [21 50]	23 (43)	36 (9) [22 50]
BD	8	UTO	SRPBS	111 (50)	25 (11) [19 60]	33 (64)	33 (10) [19 56]
BD	9	Chicago	BSNIP2	65 (40)	35 (10) [19 58]	45 (44)	28 (10) [18 59]

Supplementary Table 5. Summary of MRI acquisition details for each site.

Diagnosis	**Site**	**SBM index**	**VBM index**	**Dataset**	**Field strength (T)**	**Scanner brand**	**Scanner model**	**Voxel measures (mm)**	**Voxel volume (mm3)**
AD	AIBL-2	1	1	AIBL	3	SIEMENS	TrioTim	1x1x1.2	1.2
AD	Harmonisation	2	2	Harmonisation	3	SIEMENS	TrioTim	1x1x1	1
AD	MIRIAD	3	7	MIRIAD	1.5	GE	Signa	1x1x1.5	1.5
AD	OASIS3-3	4	3	OASIS3	1.5	SIEMENS	TrioTim	1x1x1	1
AD	OASIS3-4	5	4	OASIS3	1.5	SIEMENS	TrioTim	1x1x1	1
AD	OASIS3-5	6	5	OASIS3	3	SIEMENS	Biograph	1.05x1.05x1.2	1.323
AD	OASIS4	7	6	OASIS4	3	SIEMENS	Skyra	1.055x1.055x1.1	1.2243
SCZ	AIS	1	2	AIS	3	SIEMENS	Verio	1x1x1	1
SCZ	BrainGluSchi	2	4	BrainGluSchi	3	SIEMENS	TrioTim	1x1x1	1
SCZ	Baltimore	3	3	BSNIP	3	SIEMENS	TrioTim	1x1x1.2	1.2
SCZ	Boston2	4		BSNIP	3	SIEMENS	Verio	1x1x1.2	1.2
SCZ	Dallas2	5	7	BSNIP	3	Philips		1x1x1.2	1.2
SCZ	Hartford2	6		BSNIP	3	SIEMENS	Allegra	1x1x1.2	1.2
SCZ	Boston1	7	14	BSNIP2	3	GE	Discovery MR750w	1x1x1.2	1.2
SCZ	Chicago	8	15	BSNIP2	3	Philips		1x1x1.2	1.2
SCZ	Dallas1	9	16	BSNIP2	3	Philips		1x1x1.2	1.2
SCZ	Georgia	10		BSNIP2	3	GE	Signa HDxt	1x1x1.2	1.2
SCZ	Hartford1	11		BSNIP2	3	SIEMENS	Skyra	1x1x1.2	1.2
SCZ	COBRE	12	6	COBRE	3	SIEMENS	Trio	1x1x1	1
SCZ	DSD	13		DSD	3	SIEMENS	Prisma	1x1x1	1
SCZ	HCP-EP	14	8	HCP-EP	3	SIEMENS	Prisma	0.8x0.8x0.8	0.512
SCZ	MCIC-A	15	1	MCIC	1.5	SIEMENS	Sonata	0.625x0.625x1.5	0.5859
SCZ	MCIC-C	16	5	MCIC	3	SIEMENS	Trio	0.625x0.625x1.6	0.625
SCZ	MCIC-D	17		MCIC	1.5	SIEMENS		0.625x0.625x1.5	0.5859
SCZ	MICCD	18	11	MICCD	3	SIEMENS	TrioTim	1x1x1	1
SCZ	Speech	19	17	Speech	3	Philips	Ingenia	1x1x1	1

SCZ	KTT	20	9	SRPBS	3	SIEMENS	Trio	0.9375x0.9375x1.0	0.8789
SCZ	KUT	21	10	SRPBS	3	SIEMENS	TrioTim	0.9375x0.9375x1.0	0.8789
SCZ	UTO	22	13	SRPBS	3	GE	Discovery MR750w	1x1x1.2	1.2
SCZ	EMOSCZ	23	12	EMOSCZ	3	SIEMENS	BiographÂ	1x1x1	1
SCZ	UCLA1	24		UCLA	3	SIEMENS	Trio	1x1x1	1
SCA	Baltimore	1	1	BSNIP	3	SIEMENS	TrioTim	1x1x1.2	1.2
SCA	Dallas2	2	2	BSNIP	3	Philips		1x1x1.2	1.2
SCA	Hartford2	3		BSNIP	3	SIEMENS	Allegra	1x1x1.2	1.2
SCA	Boston1	4		BSNIP2	3	GE	Discovery MR750w	1x1x1.2	1.2
SCA	Chicago	5	3	BSNIP2	3	Philips		1x1x1.2	1.2
SCA	Dallas1	6	4	BSNIP2	3	Philips		1x1x1.2	1.2
SCA	Georgia	7	5	BSNIP2	3	GE	Signa HDxt	1x1x1.2	1.2
SCA	Hartford1	8	6	BSNIP2	3	SIEMENS	Skyra	1x1x1.2	1.2
ASD	USM	1	5	ABIDEI	3	SIEMENS	TrioTim	1x1x1.2	1.2
ASD	BNI	2	1	ABIDEII	3	Philips		1x1x1.2	1.2
ASD	ASD45	3	2	ASD45	3	GE	Discovery MR750w	0.8x0.8x0.8	0.512
ASD	IDAUT	4	3	IDAUT	3	Philips	Achieva	1x1x1	1
ASD	SWA	5	4	SRPBS	3	SIEMENS	Verio	1x1x1	1
MDD	MBBP	1	4	MBBP	3	SIEMENS	Skyra	1x1x1	1
MDD	Myelin	2	5	Myelin	3	SIEMENS	Prisma	0.8x0.8x0.8	0.512
MDD	RD	3	6	RD	3	Philips	Ingenia	1x1x1	1
MDD	COI	4	1	SRPBS	3	SIEMENS	Verio	1x1x1	1
MDD	HKH	5	2	SRPBS	3	SIEMENS	Symphon	1x1x1	1
MDD	HUH	6	3	SRPBS	3	GE	Signa HDxt	1x1x1	1
MDD	UTO	7	7	SRPBS	3	GE	Discovery MR750w	1x1x1.2	1.2
MDD	YoDA	8	8	YoDA	3	GE	Signa Excite	0.94x0.94x1	0.8836
BD	Baltimore	1	1	BSNIP	3	SIEMENS	TrioTim	1x1x1.2	1.2
BD	Boston2	2		BSNIP	3	SIEMENS	Verio	1x1x1.2	1.2
BD	Dallas2	3	2	BSNIP	3	Philips		1x1x1.2	1.2
BD	Hartford2	4		BSNIP	3	SIEMENS	Allegra	1x1x1.2	1.2
BD	Chicago	5	9	BSNIP2	3	Philips		1x1x1.2	1.2
BD	DSD	6		DSD	3	SIEMENS	Prisma	1x1x1	1
BD	MRITDCS	7	3	MRITDCS	3	SIEMENS	Prisma	1x1x1	1
BD	MICCD	8	4	MICCD	3	SIEMENS	TrioTim	1x1x1	1
BD	PARDIP1	9	5	PARDIP	3	Philips		1x1x1.2	1.2
BD	PARDIP2	10		PARDIP	3	GE	Signa HDxt	1x1x1.2	1.2
BD	SHSCBV	11		SHSCBV	3	SIEMENS	TrioTim	0.9375x0.9375x0.9	0.791
BD	UTO	12	8	SRPBS	3	GE	Discovery MR750w	1x1x1.2	1.2
BD	Transdiagnostic2	13	6	TCP	3	SIEMENS	Prisma	1.2x1.2x1.2	1.728
BD	UCLA1	14	7	UCLA	3	SIEMENS	Trio	1x1x1	1

2 Supplementary Figures

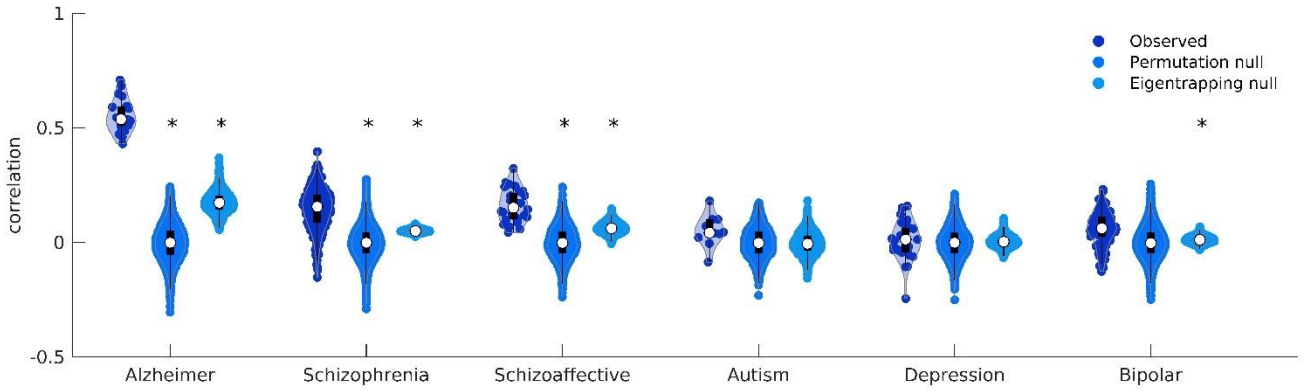

Supplementary Fig. 1|**Cross-site consistency (CSC) of site-specific left hemisphere z-maps quantified with SBM.** Distributions of pair-wise CSCs between observed site-specific z-maps, along with the corresponding distributions of the median CSCs obtained using a permutation null test[40] and a spatially autocorrelated null model[39]. White circles represent the median, black boxes show the interquartile range (IQR), and whiskers extend to the last non-outlier data points within ±1.5×IQR. Asterisks mark the disorders where the observed median CSC is significantly different from the null distribution ($p < 0.05$).

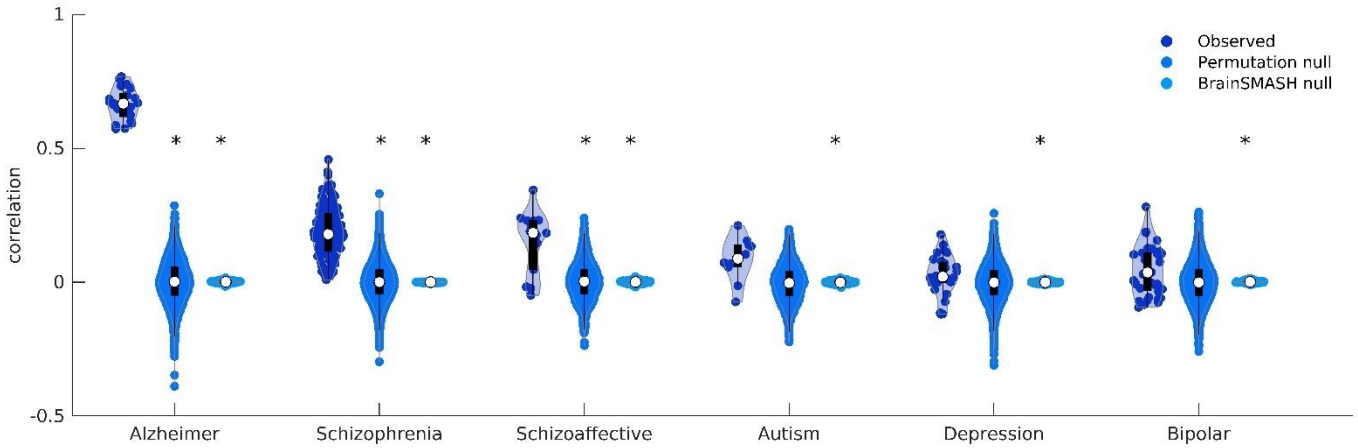

Supplementary Fig. 2|**Cross-site consistency (CSC) of site-specific left hemisphere t-maps quantified with VBM.** Distributions of pair-wise CSCs between observed site-specific t-maps, along with the corresponding distributions of the median CSCs obtained using a permutation null test[40] and a spatially autocorrelated null model[40]. White circles represent the median, black boxes show the interquartile range (IQR), and whiskers extend to the last non-outlier data points within ±1.5×IQR. Asterisks mark the disorders where the observed median CSC is significantly different from the null distribution ($p < 0.05$).

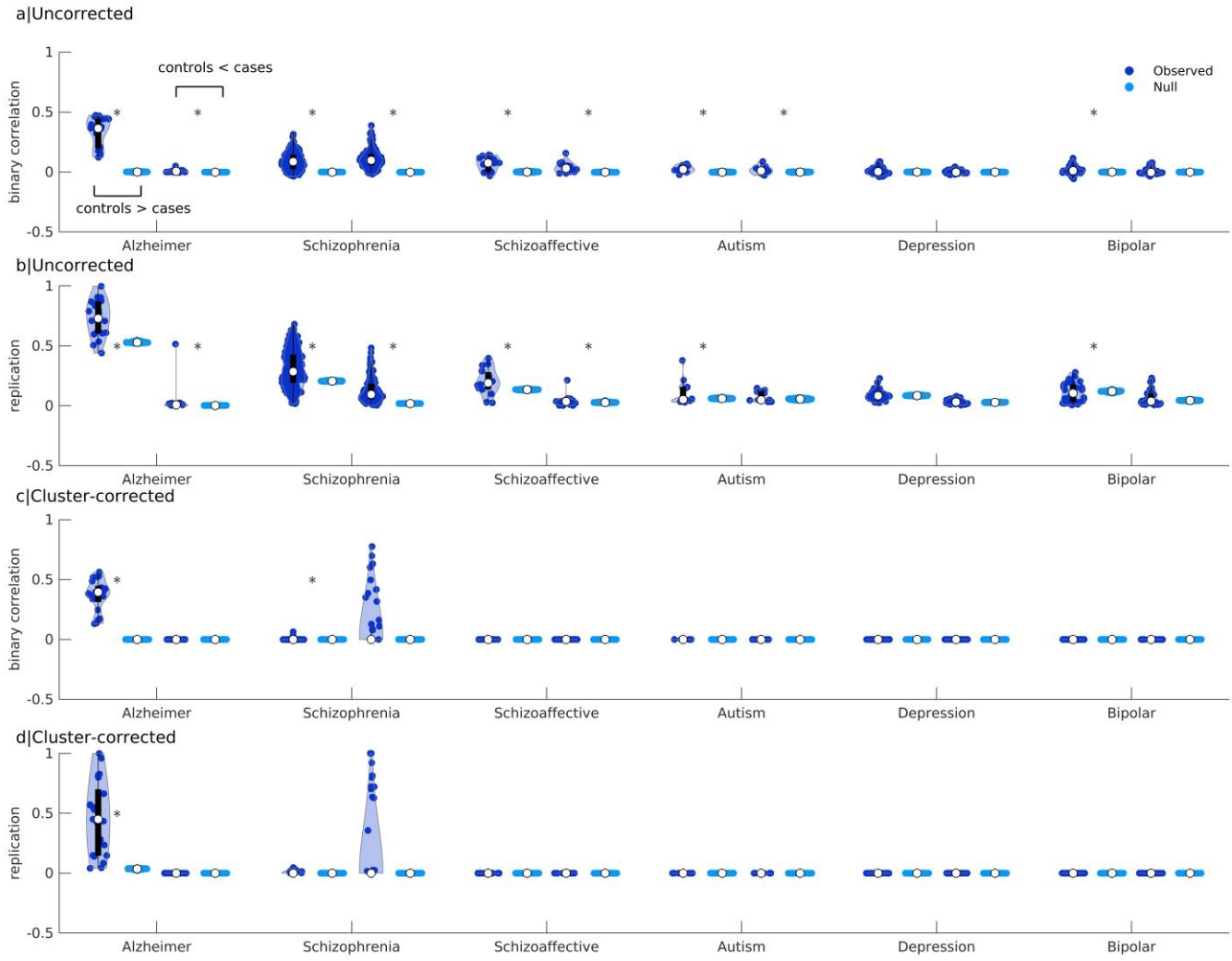

Supplementary Fig. 3|**Cross-site binary correlation and replication of site-specific thresholded *t*-maps, uncorrected and cluster-based corrected, for controls > cases and controls < cases, quantified with VBM.** Distributions of pair-wise cross-site binary correlation and replication between observed site-specific *t*-maps, along with the corresponding distributions of the cross-site binary correlation and replication medians obtained using a spatially autocorrelated null mode[40]. White circles represent the median, black boxes show the interquartile range (IQR), and whiskers extend to the last non-outlier data points within ±1.5×IQR. Asterisks mark the disorders where the observed median cross-site binary correlation or replication is significantly different from the null distribution.

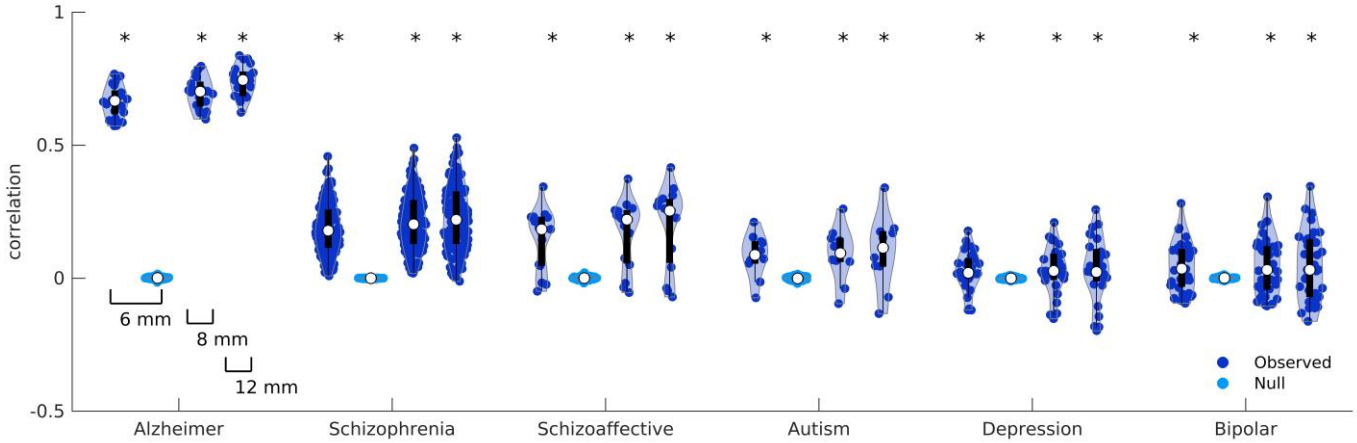

Supplementary Fig. 4|**Cross-site consistency (CSC) of site-specific *t*-maps from data preproccessed with FWHM = 6, 8, 12 mm, quantified with VBM.** Distributions of pair-wise CSCs between observed site-specific *t*-maps, along with the corresponding distributions of the CSC medians obtained using a spatially autocorrelated null model[40]. White circles represent the median, black boxes show the interquartile range (IQR), and whiskers extend to the last

non-outlier data points within ±1.5×IQR. Asterisks mark the disorders where the observed median CSC, cross-site binary correlation, or replication is significantly different from the null distribution.

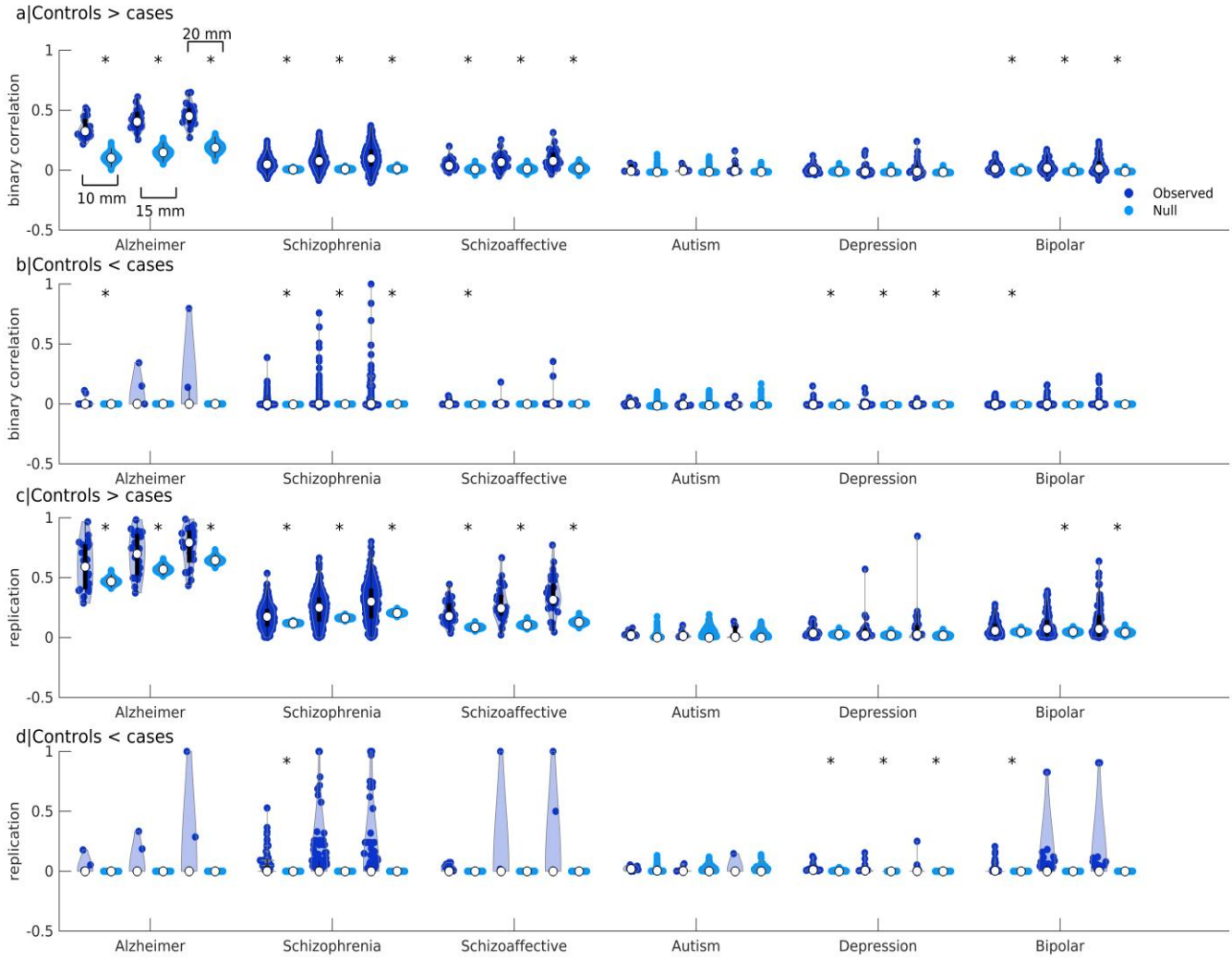

Supplementary Fig. 5| **Cross-site binary correlation and replication of site-specific left hemisphere uncorrected thresholded z-maps for controls > cases and controls < cases from data preprocessed with FWHM = 10, 15, 20 mm, quantified with SBM.** Distributions of pair-wise cross-site binary correlation and replication between observed site-specific z-maps, along with the corresponding distributions of the cross-site binary correlation and replication medians obtained using a spatially autocorrelated null model[39]. White circles represent the median, black boxes show the interquartile range (IQR), and whiskers extend to the last non-outlier data points within ±1.5×IQR. Asterisks mark the disorders where the observed median cross-site binary correlation or replication is significantly different from the null distribution.

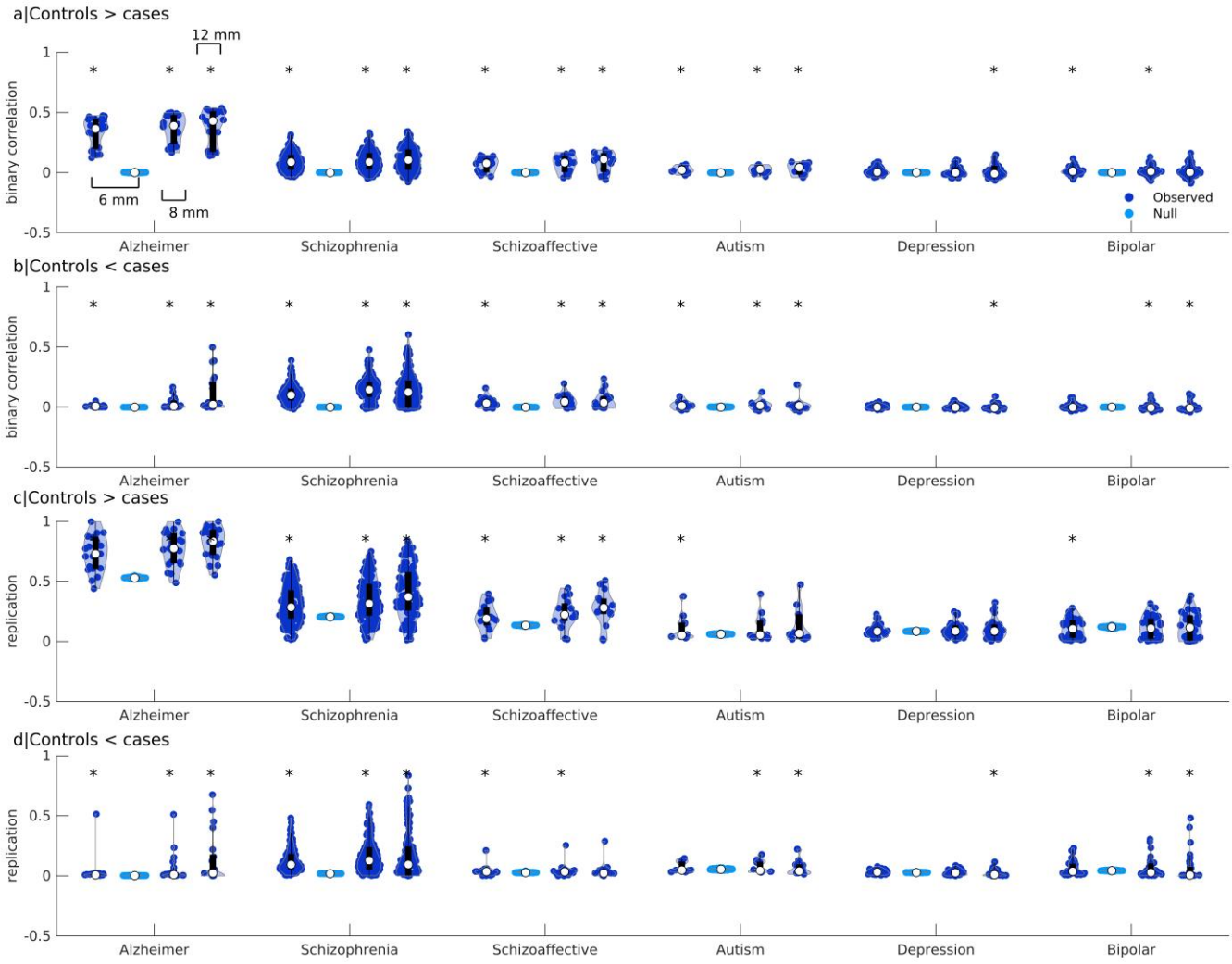

Supplementary Fig. 6| **Cross-site binary correlation and replication of site-specific uncorrected thresholded *t*-maps for controls > cases and controls < cases from data preproccessed with FWHM = 6, 8, 12 mm, quantified with VBM.** Distributions of pair-wise cross-site binary correlation and replication between observed site-specific *t*-maps, along with the corresponding distributions of the cross-site binary correlation and replication medians obtained using a spatially autocorrelated null model[40]. White circles represent the median, black boxes show the interquartile range (IQR), and whiskers extend to the last non-outlier data points within ±1.5×IQR. Asterisks mark the disorders where the observed median cross-site binary correlation and replication is significantly different from the null distribution.

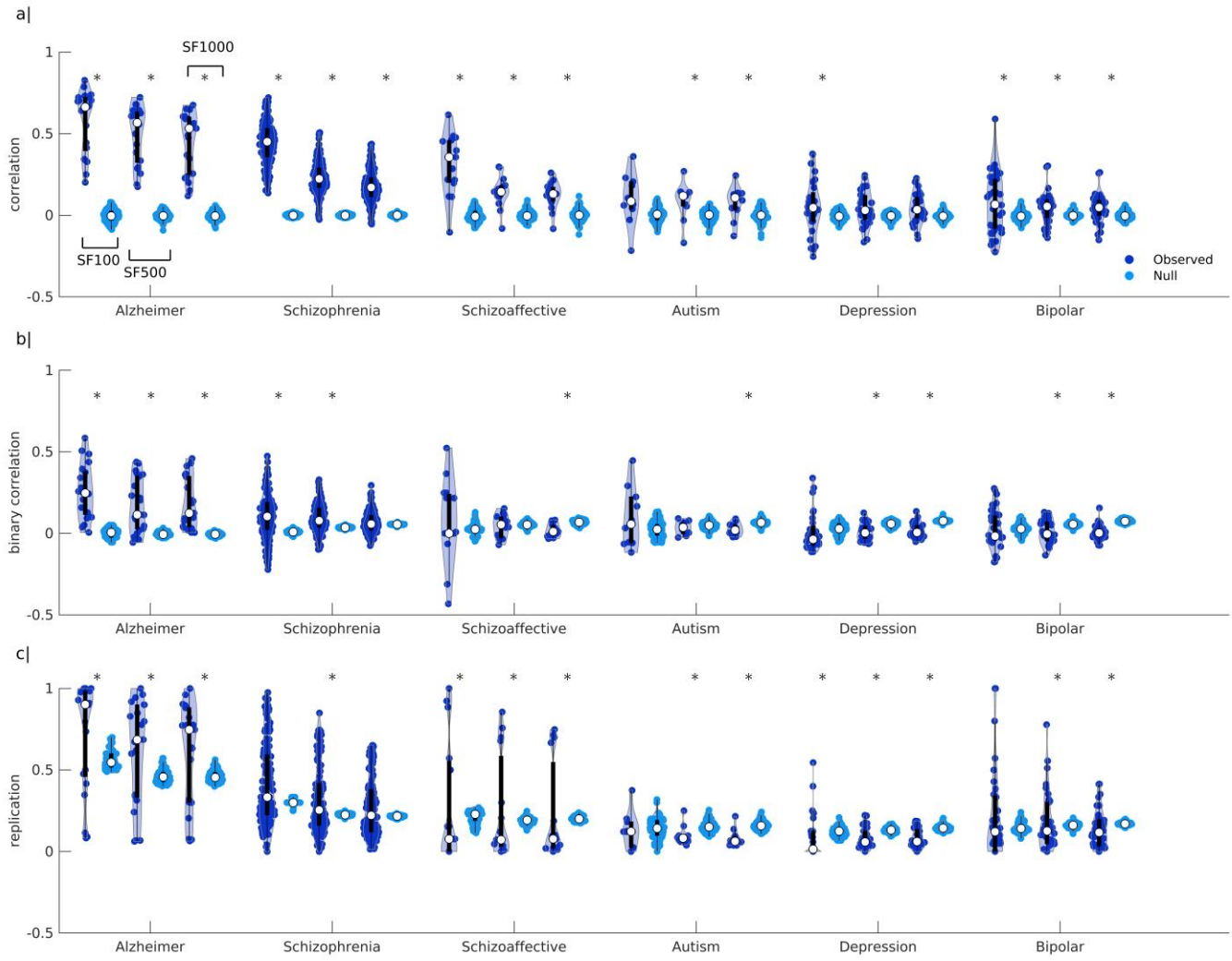

Supplementary Fig. 7|**Cross-site consistency, binary correlation, and replication of site-specific parcellated *t*-maps in Schaefer-100, Schaefer-500, and Schaefer-1000 atlases, quantified with VBM.** Distributions of pair-wise cross-site correlations, binary correlation, and replication between observed site-specific *t*-maps, along with the corresponding distributions of the cross-site correlation, binary correlation, and replication medians obtained using a spatially autocorrelated null model[40]. White circles represent the median, black boxes show the interquartile range (IQR), and whiskers extend to the last non-outlier data points within ±1.5×IQR. Asterisks mark the disorders where the observed median cross-site correlation, binary correlation, or replication is significantly different from the null distribution.

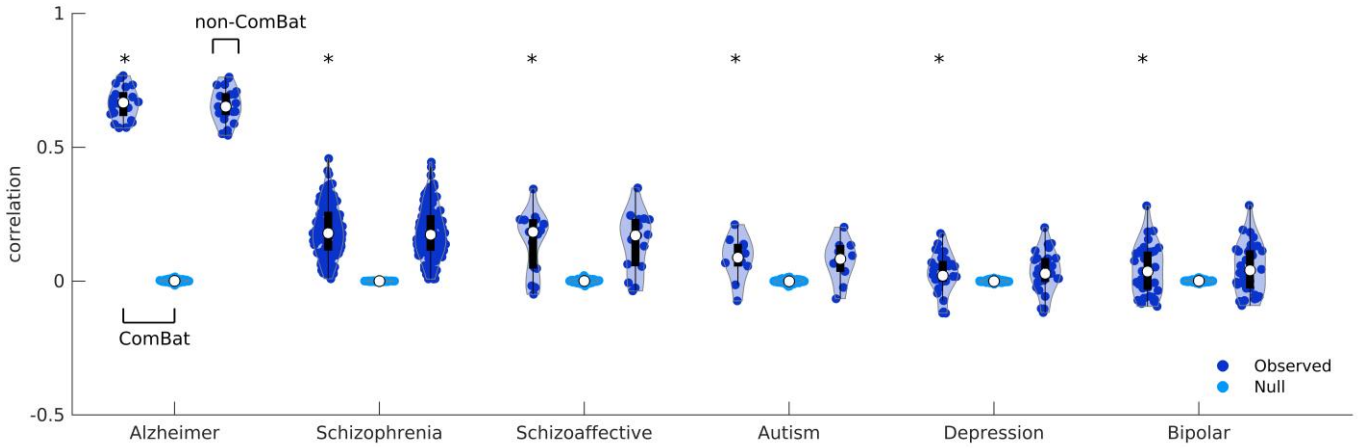

Supplementary Fig. 8| **Cross-site consistency (CSC) of site-specific *t*-maps from data preprocessed with and without ComBat, quantified with VBM.** Distributions of pair-wise CSCs between observed site-specific *t*-maps, along with the corresponding distributions of the median CSCs obtained using a spatially autocorrelated null model[40]. White circles represent the median. Black boxes show the interquartile range (IQR) and whiskers extend to the last non-outlier data points within ±1.5×IQR. Asterisks mark the disorders where the observed median CSC is significantly different from the null distribution.

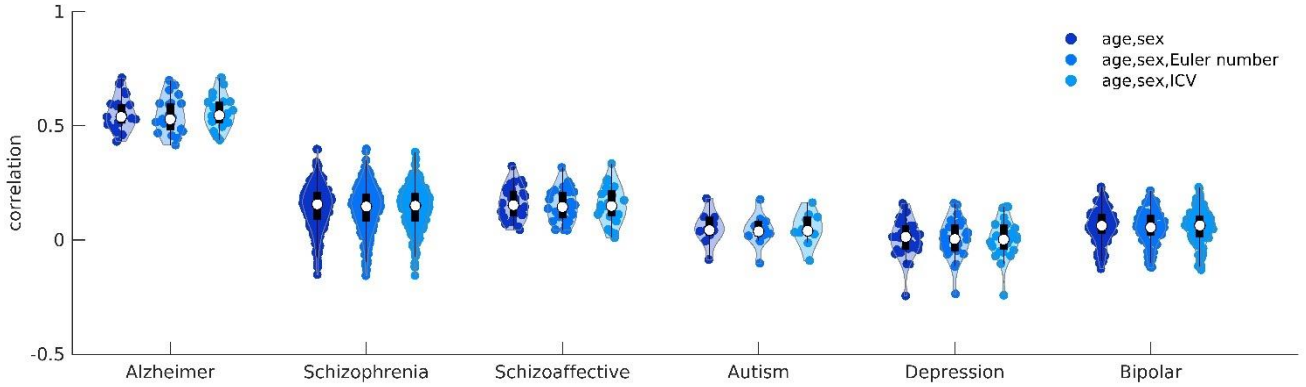

Supplementary Fig. 9| **Cross-site consistency (CSC) of site-specific left hemisphere *z*-maps from statistical analysis without and with Euler number or ICV as a covariate in addition to age and sex, quantified with SBM.** Distributions of pair-wise CSCs between observed site-specific *z*-maps without and with Euler number or ICV as a covariate in addition to age and sex. White circles represent the median, black boxes show the interquartile range (IQR), and whiskers extend to the last non-outlier data points within ±1.5×IQR.

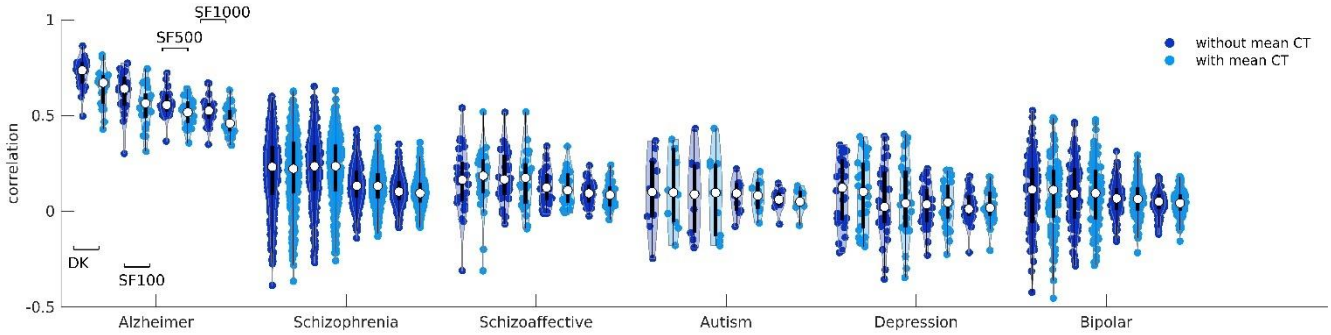

Supplementary Fig. 10| **Cross-site consistency of site-specific left hemisphere parcellated *z*-maps in DK, Schaefer-100, Schaefer-500, and Schaefer-1000 atlases without and with mean CT as a covariate, quantified with SBM.** Distributions of pair-wise cross-site correlations between observed site-specific *z*-maps without and with mean CT as a covariate. White circles represent the median, black boxes show the interquartile range (IQR), and whiskers extend to the last non-outlier data points within ±1.5×IQR.

3 References

1. Di Martino, A. *et al.* The autism brain imaging data exchange: towards a large-scale evaluation of the intrinsic brain architecture in autism. *Mol. Psychiatry* **19**, 659–667 (2014).

2. Anderson, J. S. *et al.* Decreased interhemispheric functional connectivity in autism. *Cereb. Cortex N. Y. N 1991* **21**, 1134–1146 (2011).

3. Di Martino, A. *et al.* Enhancing studies of the connectome in autism using the autism brain imaging data exchange II. *Sci. Data* **4**, 170010 (2017).

4. Rowe, C. C. *et al.* Amyloid imaging results from the Australian Imaging, Biomarkers and Lifestyle (AIBL) study of aging. *Neurobiol. Aging* **31**, 1275–1283 (2010).

5. Ellis, K. A. *et al.* The Australian Imaging, Biomarkers and Lifestyle (AIBL) study of aging: methodology and baseline characteristics of 1112 individuals recruited for a longitudinal study of Alzheimer's disease. *Int. Psychogeriatr.* **21**, 672–687 (2009).

6. Baajour, S. J. *et al.* Disordered directional brain network interactions during learning dynamics in schizophrenia revealed by multivariate autoregressive models. *Hum. Brain Mapp.* **41**, 3594–3607 (2020).

7. Tamminga, C. A. *et al.* Clinical phenotypes of psychosis in the Bipolar-Schizophrenia Network on Intermediate Phenotypes (B-SNIP). *Am. J. Psychiatry* **170**, 1263–1274 (2013).

8. Kohli, J. S., Kinnear, M. K., Martindale, I. A., Carper, R. A. & Müller, R.-A. Regionally decreased gyrification in middle-aged adults with autism spectrum disorders. *Neurology* **93**, e1900–e1905 (2019).

9. Bustillo, J. R. *et al.* Glutamatergic and Neuronal Dysfunction in Gray and White Matter: A Spectroscopic Imaging Study in a Large Schizophrenia Sample. *Schizophr. Bull.* **43**, 611–619 (2017).

10. Mayer, A. R. *et al.* Functional imaging of the hemodynamic sensory gating response in schizophrenia. *Hum. Brain Mapp.* **34**, 2302–2312 (2012).

11. Jahshan, C., Wynn, J. K., Roach, B. J., Mathalon, D. H. & Green, M. F. Effects of Transcranial Direct Current Stimulation on Visual Neuroplasticity in Schizophrenia. *Clin. EEG Neurosci.* **51**, 382–389 (2020).

12. Jacobs, G. R. *et al.* An Introduction to the Human Connectome Project for Early Psychosis. *Schizophr. Bull.* sbae123 (2024) doi:10.1093/schbul/sbae123.

13. Hilal, S. *et al.* Markers of cardiac dysfunction in cognitive impairment and dementia. *Medicine (Baltimore)* **94**, e297 (2015).

14. Chong, J. S. X. *et al.* Influence of cerebrovascular disease on brain networks in prodromal and clinical Alzheimer's disease. *Brain J. Neurol.* **140**, 3012–3022 (2017).

15. Hilal, S. *et al.* Cortical cerebral microinfarcts predict cognitive decline in memory clinic patients. *J. Cereb. Blood Flow Metab. Off. J. Int. Soc. Cereb. Blood Flow Metab.* **40**, 44–53 (2020).

16. Murray, S. O. *et al.* Sex Differences in Visual Motion Processing. *Curr. Biol. CB* **28**, 2794-2799.e3 (2018).

17. Kolodny, T., Schallmo, M.-P., Gerdts, J., Bernier, R. A. & Murray, S. O. Response Dissociation in Hierarchical Cortical Circuits: a Unique Feature of Autism Spectrum Disorder. *J. Neurosci. Off. J. Soc. Neurosci.* **40**, 2269–2281 (2020).

18. Gollub, R. L. *et al.* The MCIC collection: a shared repository of multi-modal, multi-site brain image data from a clinical investigation of schizophrenia. *Neuroinformatics* **11**, 367–388 (2013).

19. Arora, M. *et al.* Left Ventrolateral Prefrontal Cortical Activity During Reward Expectancy and Mania Risk. *JAMA Psychiatry* https://doi.org/10.1001/jamapsychiatry.2024.4216 (2025) doi:10.1001/jamapsychiatry.2024.4216.

20. Wertz, C. J. *et al.* Disconnected and Hyperactive: A Replication of Sensorimotor Cortex Abnormalities in Patients With Schizophrenia During Proactive Response Inhibition. *Schizophr. Bull.* **45**, 552–561 (2019).

21. Baranger, D. A. A. *et al.* Aberrant levels of cortical myelin distinguish individuals with unipolar depression from healthy controls. 2021.02.25.21252472 Preprint at https://doi.org/10.1101/2021.02.25.21252472 (2021).

22. LaMontagne, P. J. *et al.* OASIS-3: Longitudinal Neuroimaging, Clinical, and Cognitive Dataset for Normal Aging and Alzheimer Disease. *medRxiv* https://doi.org/10.1101/2019.12.13.19014902 (2019) doi:10.1101/2019.12.13.19014902.

23. Koenig, L. N. *et al.* Select Atrophied Regions in Alzheimer disease (SARA): An improved volumetric model for identifying Alzheimer disease dementia. *NeuroImage Clin.* **26**, 102248 (2020).

24. Lutz, O. *et al.* 965. Investigating Brain Structure Across Bipolar Disorder Subtypes: Findings from the Psychosis Affective Research Domain Intermediate Phenotypes (PARDIP) Study. *Biol. Psychiatry* **81**, S390–S391 (2017).

25. Meyhoefer, I. *et al.* Evidence from comprehensive independent validation studies for smooth pursuit dysfunction as a sensorimotor biomarker for psychosis. *Sci. Rep.* **14**, 13859 (2024).

26. Bezmaternykh, D. D. *et al.* Brain Networks Connectivity in Mild to Moderate Depression: Resting State fMRI Study with Implications to Nonpharmacological Treatment. *Neural Plast.* **2021**, 8846097 (2021).

27. Tanaka, S. C. *et al.* A multi-site, multi-disorder resting-state magnetic resonance image database. *Sci. Data* **8**, 227 (2021).

28. Yahata, N. *et al.* A small number of abnormal brain connections predicts adult autism spectrum disorder. *Nat. Commun.* **7**, 11254 (2016).

29. Nakahara, S., Matsumoto, M. & van Erp, T. G. M. Hippocampal subregion abnormalities in schizophrenia: A systematic review of structural and physiological imaging studies. *Neuropsychopharmacol. Rep.* **38**, 156–166 (2018).

30. Moran, E. K., Culbreth, A. J. & Barch, D. M. Ecological momentary assessment of negative symptoms in schizophrenia: Relationships to effort-based decision making and reinforcement learning. *J. Abnorm. Psychol.* **126**, 96–105 (2017).

31. Eisenstein, S. A. *et al.* Preliminary evidence that negative symptom severity relates to multilocus genetic profile for dopamine signaling capacity and D2 receptor binding in healthy controls and in schizophrenia. *J. Psychiatr. Res.* **86**, 9–17 (2017).

32. Chopra, S. *et al.* The Transdiagnostic Connectome Project: a richly phenotyped open dataset for advancing the study of brain-behavior relationships in psychiatry. 2024.06.18.24309054 Preprint at https://doi.org/10.1101/2024.06.18.24309054 (2024).

33. Poldrack, R. A. *et al.* A phenome-wide examination of neural and cognitive function. *Sci. Data* **3**, 160110 (2016).

34. UCLA Consortium for Neuropsychiatric Phenomics LA5c Study - OpenNeuro. https://openneuro.org/datasets/ds000030/versions/1.0.0.

35. Davey, C. G. *et al.* The addition of fluoxetine to cognitive behavioural therapy for youth depression (YoDA-C): a randomised, double-blind, placebo-controlled, multicentre clinical trial. *Lancet Psychiatry* **6**, 735–744 (2019).

36. Davey, C. G., Cearns, M., Jamieson, A. & Harrison, B. J. Suppressed activity of the rostral anterior cingulate cortex as a biomarker for depression remission. *Psychol. Med.* **53**, 2448–2455 (2023).

37. Malone, I. B. *et al.* MIRIAD—Public release of a multiple time point Alzheimer's MR imaging dataset. *NeuroImage* **70**, 33–36 (2013).

38. Soler-Vidal, J. *et al.* Brain correlates of speech perception in schizophrenia patients with and without auditory hallucinations. *PloS One* **17**, e0276975 (2022).

39. Koussis, N. C. *et al.* Generation of surrogate brain maps preserving spatial autocorrelation through random rotation of geometric eigenmodes. *Imaging Neurosci.* https://doi.org/10.1162/IMAG.a.71 (2025) doi:10.1162/IMAG.a.71.

40. Burt, J. B., Helmer, M., Shinn, M., Anticevic, A. & Murray, J. D. Generative modeling of brain maps with spatial autocorrelation. *NeuroImage* **220**, 117038 (2020).

41. Glerean, E. *et al.* Reorganization of functionally connected brain subnetworks in high-functioning autism. *Hum. Brain Mapp.* **37**, 1066–1079 (2016).